



Published in final edited form as:

*Ann N Y Acad Sci*. 2018 April ; 1418(1): 106–117. doi:10.1111/nyas.13557.

## Cardioprotective effects of dietary rapamycin on adult female C57BLKS/J-*Lepr<sup>db</sup>* mice

Peter C. Reifsnyder<sup>1</sup>, Sergey Ryzhov<sup>2</sup>, Kevin Flurkey<sup>1</sup>, Rea P. Anunciado-Koza<sup>2</sup>, Ian Mills<sup>2</sup>, David E. Harrison<sup>1</sup>, and Robert A. Koza<sup>2</sup>

<sup>1</sup>The Jackson Laboratory, Bar Harbor, Maine

<sup>2</sup>Center for Molecular Medicine, Maine Medical Center Research Institute, Scarborough, Maine

### Abstract

Rapamycin (RAPA), an inhibitor of mTORC signaling, has been shown to extend life span in mice and other organisms. Recently, animal and human studies have suggested that inhibition of mTORC signaling can alleviate or prevent the development of cardiomyopathy. In view of this, we used a murine model of type 2 diabetes (T2D), BKS-*Lepr<sup>db</sup>*, to determine whether RAPA treatment can mitigate the development of T2D-induced cardiomyopathy in adult mice. Female BKS-*Lepr<sup>db</sup>* mice fed diet supplemented with RAPA from 11 to 27 weeks of age showed reduced weight gain and significant reductions of fat and lean mass compared with untreated mice. No differences in plasma glucose or insulin levels were observed between groups; however, RAPA-treated mice were more insulin sensitive ( $P < 0.01$ ) than untreated mice. Urine ACR was lower in RAPA-treated mice, suggesting reduced diabetic nephropathy and improved kidney function. Echocardiography showed significantly reduced left ventricular wall thickness in mice treated with RAPA compared with untreated mice ( $P = 0.02$ ) that was consistent with reduced heart weight/tibia length ratios, reduced myocyte size and cardiac fibrosis measured by histomorphology, and reduced mRNA expression of *Coll1a1*, a marker for cardiomyopathy. Our results suggest that inhibition of mTORC signaling is a plausible strategy for ameliorating complications of obesity and T2D, including cardiomyopathy.

### Keywords

rapamycin; diabetes; obesity; cardiomyopathy; mTORC

### Introduction

Numerous studies have shown that inhibition of the mTORC (mechanistic target Of rapamycin complex) pathway by rapamycin (RAPA) can lead to increased longevity in mice as well as other organisms, such as yeast, *Drosophila*, and *Caenorhabditis elegans*.<sup>1–5</sup> Positive effects attributed to RAPA inhibition of mTORC include reduced body weight and adiposity,<sup>6–8</sup> protection against development of diabetic nephropathy,<sup>9,10</sup> and improvement

Address for correspondence: rkoza@mmc.org.

The authors declare that there are no conflicts of interest.

in hepatic function<sup>11–14</sup> However, RAPA inhibition of mTORC can lead to exacerbated hyperglycemia, glucose intolerance, and hyperlipidemia in both murine models<sup>8,15,16</sup> and renal transplant and cancer patients treated with immunosuppressive rapamycin analogs.<sup>17,18</sup> Although we have not examined RAPA inhibition of mTORC1 or mTORC2 in our studies, it has been suggested by others that negative RAPA-mediated effects on pancreatic islets and glucose homeostasis occur via inhibition of the mTORC2 complex, whereas positive benefits that promote longevity derive from RAPA inhibition of the mTORC1 complex.<sup>19,20</sup> Cardioprotective effects of mTOR inhibition have also been shown to occur primarily via attenuation of mTORC1, whereas inhibition of mTORC2 with RICTOR or the pharmacological mTORC1/mTORC2 inhibitor Torin 1 can lead to further exacerbated cardiomyocyte apoptosis and tissue damage following myocardial infarction<sup>21</sup> AKT1 substrate 1 (AKT1S), also known as PRAS40, has been shown to inhibit mTORC1 and prevent the development of both hepatic insulin sensitivity and diabetic cardiomyopathy in mice.<sup>21,22</sup> Infusion of diabetic adult male *db/db* mouse hearts with rapamycin following ischemic injury at the onset of reperfusion was shown to significantly reduce myocardial infarct size, possibly via a STAT3-dependent mechanism.<sup>23</sup> A more recent study suggests that intracardiac injection of rapamycin in mice following myocardial ischemia can reduce myocardial infarct size by selective activation of mTORC2 and ERK and inhibition of the mTORC1 and p38 pathways.<sup>24</sup>

Because of the detrimental effects of RAPA treatment on glucose tolerance and pancreatic insulin secretion and content,<sup>25</sup> it seems likely that RAPA treatment would worsen diabetic outcomes for murine models of obesity and type 2 diabetes (T2D). Surprisingly, studies showed that RAPA treatment of obese T2D-prone BKS-*Lep<sup>db</sup>* mice did not further exacerbate hyperglycemia, and the mice showed markedly improved insulin sensitivity, reduced adiposity, and elevated adipose tissue fatty acid oxidation.<sup>26</sup> However, a recent study showed that long-term dietary RAPA treatment reduced life span of BKS-*Lep<sup>db</sup>* mice compared with control mice and is the first example showing reduced longevity due to RAPA treatment on a strain of mice.<sup>27</sup> Furthermore, a survey of five mouse strains prone to development of T2D suggests that worsening of hyperglycemia following RAPA treatment is strain dependent and associated with RAPA-mediated depletion of stored pancreatic insulin content.<sup>28</sup>

Studies have shown that RAPA inhibition of mTORC can mitigate the development of hypertrophic cardiomyopathy in genetically susceptible rodent models<sup>29,30</sup> and uremic cardiomyopathy in partially nephrectomized rats treated with cardioprotective steroids.<sup>31</sup> In addition, studies showed that male diabetic BKS-*Lep<sup>db</sup>* mice treated with RAPA for 28 days showed marked improvement in cardiac phenotypes compared with control mice.<sup>32</sup> In this current study, we will examine the effects of chronic low-dose dietary administration of RAPA on both the longitudinal measurements of diabetes-related parameters and the development of cardiomyopathy in female diabetic mice. Potential effects of long-term RAPA treatment on life span of both female and male BKS-*Lep<sup>db</sup>* mice will also be evaluated. Results from these studies will further establish the effectiveness of RAPA-mediated inhibition of mTORC as a strategy for ameliorating and/or preventing cardiovascular complications concomitant with obesity and T2D.

## Materials and methods

### Animals, diets, and caging

Forty female and 20 male BKS.Cg-*Dock7<sup>tm</sup>* +/+ *Lep<sup>rdb</sup>*/J mice (BKS-*Lep<sup>rdb</sup>*, JAX® Stock Number 642, <https://www.jax.org/strain/000642>) were received at 8 weeks of age from the Jackson Laboratory (Bar Harbor, Maine) production barrier facility into the investigator's mouse room at the Jackson Laboratory (records of pathogens tested are available in health status reports for room D1 at <http://jaxmice.jax.org/genetichealth/index.html>). The mouse room was maintained on a light/dark cycle of 12 h, ~ 25 °C, and 40–50% humidity; all mice were housed with pine shaving bedding and acidified water. The BKS-*Lep<sup>rdb</sup>* mice were housed in weaning pens (5 mice per pen) and were maintained ad libitum on chow diet containing 4% fat (5LG6; PMI, Brentwood, MO). For the sacrifice cohort, at 11 weeks of age, 10 females were switched to 11% fat chow diet (5LA0; PMI), and 10 females were switched to 5LA0 diet containing 14 ppm encapsulated rapamycin. For the life span cohort, at 15 weeks of age, 10 females and 10 males were switched to 5LA0 ± rapamycin diets. The concentration of rapamycin in the diet was chosen because it had been previously determined to extend life span in mice.<sup>1</sup> The encapsulation vehicle Eudragit S100 is biologically inert and passes through the gut unchanged. It is classified by the U.S. Food and Drug Administration as GRAS (generally recognized as safe) and is used in pharmaceuticals to target drugs to the gut.

### Phenotyping

All mice were weighed every 2 weeks. Mice were bled every 4 weeks via the retro-orbital sinus. Mice were fasted for 3–4 hours in a clean cage from 7:00 a.m. to 10–11:00 a.m. before blood collection. This represents a fed blood draw, as mice would not normally feed during this period, but prevents variability in the values due to any morning food ingestion. Plasma glucose (PG) values were measured by glucometer (OneTouch, LifeScan, Inc.). Plasma insulin (PI) values were measured from the same blood draw as PG by ELISA (Meso Scale Discovery, Gaithersburg, MD). Spot urine samples were collected over three consecutive days at 22 weeks of age, and albumin/creatinine ratios (ACRs) were determined using the UniCel DxC 600 Synchron clinical system (Beckman Coulter, Inc., Brea, CA). Insulin tolerance test (ITT) was performed at 24 weeks of age. Mice were fasted in the morning from 8:00 to 11:00 a.m. before injection with 1.5 U/kg humulin (Eli Lilly, Indianapolis, IN). Lean and fat mass was measured at 24 weeks of age by Echo MRI 3-in-1 whole-body NMR-based analyzer system (EchoMRI, Houston, TX, USA). Echocardiography was performed on isoflurane anesthetized mice at 25 weeks of age using a Vivo 2100 (Visual Sonic, Toronto, Ontario, Canada). Four 8-week-old C57BL/6J females were used as controls for echocardiography measurements (B6; the Jackson Laboratory; JAX® Stock Number 664). At sacrifice at 27 weeks of age, mice were bled from the retro-orbital sinus before euthanasia by cervical dislocation. The heart was collected and flushed with 0.2% heparin in PBS before being weighed. The atrium was removed from the heart, and a slice of the ventricle was collected and placed into neutral buffered formalin (NBF). The remainder of the ventricle was frozen in liquid nitrogen. Pancreas was collected and frozen in liquid nitrogen for measurement of pancreatic insulin content. Adipose tissue fat pads were excised and weighed, and tibia length was measured. Glucose, triglycerides,

alanine aminotransferase (ALT), aspartate aminotransferase (AST), blood urea nitrogen (BUN), creatinine kinase (CK), thyroxine (T4), and thyroxine uptake % (TUP%) were determined from serum collected at termination using the UniCel DxH 600 Synchron clinical system. All procedures were approved by the Animal Care and Use Committee of the Jackson Laboratory (Animal Use Summary #99084) and comply with guidelines in accordance with National Institutes of Health.

### Gene expression analyses

Heart tissue was isolated from euthanized mice and quickly frozen in liquid nitrogen. Tissue was pulverized in liquid nitrogen using a mortar and pestle before being homogenized in TriReagent (Molecular Research Center, Inc.). RNA was purified using RNeasy Mini Kit and RNase-free DNase I (Qiagen). Isolated RNA was protected from RNase contamination with SUPERase-In (Life Technologies), and RNA quantity and quality was determined using a Nanodrop 1000 spectrophotometer. Quantitative reverse transcription PCR was performed using total RNA with specific primers and probes designed using Primer Express software v3.0.1 (Life Technologies) essentially as previously described,<sup>33</sup> except that a BioRad CFX Real-Time System was used for analyses. Gene expression data were normalized to TATA-box binding protein (*Tbp*).

### Statistics

ANOVA (JMP, SAS Institute, Inc., Cary, NC) was used for comparisons of treatment effects. Repeated measures MANOVA (JMP) was used to assess treatment differences in body weight, plasma glucose, and plasma insulin over the course of the experiment. Cardiomyocyte length was histologically determined in hematoxylin and eosin (H&E)-stained left ventricular heart sections by measuring 15 cardiomyocytes in each of six different field images (~ 90 cardiomyocytes per heart) using ImageJ. Masson's trichrome staining for interstitial fibrosis was quantified in 3 field images for each left ventricular heart section using ImageJ and represented as percent coverage. The generation of field images, cardiomyocyte length determination, and quantification of fibrosis were performed using randomized de-identified slides to prevent bias in measurements. Statistical calculations were performed using GraphPad Prism software V.6 and Microsoft Excel 2010. Differences between two groups were calculated using two-tailed unpaired parametric *t*-test with confidence level at 95%. Significance among multiple groups was calculated with ordinary one-way ANOVA followed by Tukey's multiple comparisons test with an  $\alpha$  of 0.5. Significance between groups in longitudinal studies was measured using 2-way ANOVA with Sidak's multiple comparisons test. Data is presented as the mean  $\pm$  SEM with a  $P < 0.05$  considered to be significant.

## Results

### Bodyweight and composition of control and RAPA-treated female BKS-*Lepr<sup>db</sup>* mice

Although bodyweights of two cohorts of 11-week-old female BKS-*Lepr<sup>db</sup>* mice were comparable (control 47.69 g vs. RAPA-treated 47.36 g) before initiation of dietary rapamycin (RAPA) treatment, they quickly diverged, with RAPA-treated mice showing significant reductions in weight gain after 4 weeks of treatment (Fig. 1A) compared with

untreated control mice. Bodyweights of RAPA-treated mice were almost 10% lower after being fed the diet for 8 weeks (19 weeks of age) compared with controls. Body composition analyses of mice using NMR at 23 weeks of age showed that RAPA-treated mice had significantly reduced lean and fat mass compared with controls (Fig. 1B), with fat mass accounting for ~ 77% of the RAPA-mediated weight loss. A compensatory reduction of lean mass at ~ 25% the amount of fat mass has been shown to be commonly associated with weight loss.<sup>34</sup> Weight loss in RAPA-treated mice was reflected by significant reductions in subcutaneous inguinal and scapular adipose tissue depot weights compared with controls (Fig. 1C and 1D); however, visceral gonadal adipose tissue depots showed small but significantly increased weight (Fig. 1E) in the RAPA-treated versus control mice.

### Glucose and insulin parameters of control and RAPA-treated female BKS-*Lepr<sup>db</sup>* mice

Although BKS-*Lepr<sup>db</sup>* female mice become hyperglycemic and hyperinsulinemic at an early age,<sup>35</sup> non-fasting plasma glucose and insulin measured in mice after a brief 3–4 h withdrawal of food at 4-week intervals (from 11–23 weeks) showed no significant differences between control and RAPA-treated mice (Fig. 2A and 2B). The increase of plasma glucose (Fig. 2A) during the 12-week study corresponded with progressively lower plasma insulin levels (Fig. 2B), suggesting that pancreatic beta cells are being depleted over time, which is a common feature of BKS-*Lepr<sup>db</sup>* mice. An ITT performed on mice at 24 weeks of age showed that RAPA-treated mice were significantly more insulin sensitive than control mice (Fig. 2C), suggesting improved glucose homeostasis. Pancreatic insulin content (PIC) was unaffected by RAPA treatment (Fig. 2D).

### Serum and urine analyses of control and RAPA-treated female BKS-*Lepr<sup>db</sup>* mice

A screen of metabolites and markers from serum obtained from non-fasted mice before termination at 27 weeks of age showed significantly lower glucose (GLU) and aspartate aminotransferase (AST) and increased serum thyroxine (T4) in non-fasted RAPA-treated compared to control mice (Table 1). Although the levels of non-fasting glucose measured in serum using the UniCel Dx C 600 Synchron clinical system were modestly elevated compared with previous measurements of plasma glucose using a glucometer (Fig. 2A), they consistently showed reduced circulating glucose levels in the RAPA-treated mice indicative of more efficient glucose clearance. The significant reductions of AST and a trend for reduced levels of alanine aminotransferase (ALT) in serum of RAPA-treated mice suggest improved hepatic health compared with control-fed mice. The small but significant ~ 12% increase of T4 in serum of RAPA-treated mice could indicate slightly improved thyroid function compared with control mice; however, levels were generally consistent to what is normally observed for 18-week-old female C57BLKS/J mice (JAX; Phenome Database; <https://phenome.jax.org/measureset/24476>). In addition, thyroxine uptake (TUP; %) was consistent between control and RAPA-treated mice, suggesting no differences in thyroid hormone-binding capacity between treatment groups. No significant differences were observed in serum triglycerides (TRIG), blood urea nitrogen (BUN), or creatinine kinase (CK) between groups. Analyses of urine albumin/creatinine ratio (ACR) showed significantly higher ACR in control compared with RAPA-treated mice ( $356 \pm 64$  vs.  $168 \pm 36$ ;  $P = 0.033$ ), which suggests that RAPA treatment reduces the onset of diabetic nephropathy, as indicated in previous studies.<sup>36</sup>

### Cardiac phenotype of control and RAPA-treated female BKS-*Lepr<sup>db</sup>* mice

Echocardiography performed on control and RAPA-treated BKS-*Lepr<sup>db</sup>* mice at 25 weeks of age showed significantly reduced (~ 19%;  $P = 0.016$ ) left ventricular posterior wall thickness and diastole (LVPWd) in RAPA-treated compared with control mice (Fig. 3A). Surprisingly, LVPWd in RAPA-treated BKS-*Lepr<sup>db</sup>* mice was comparable to that observed in a cohort of age-matched female C57BL/6J mice (Fig. 3A). In addition, hearts excised from RAPA-treated mice at 27 weeks of age were ~ 17% smaller (Fig. 3B;  $P = 0.0010$ ) than those from control mice when normalized to tibia length. However, no apparent differences in percent ejection fraction (Fig. 3C) or fractional shortening (Fig. 3D) were observed between treatment groups. Histological evaluation of cardiomyocyte length in left ventricular cross sections showed significantly reduced cardiomyocyte size in the RAPA-treated mice compared with controls (Fig. 4A and 4B;  $P = 0.025$ ) and is consistent with the echocardiography and heart weight data. Gene expression analyses of RNA extracted from heart tissue showed significant reductions of both *Col1a1* and *Gata4* (Fig. 5A and 5B) in RAPA-treated compared with control mice. Elevated expression of profibrotic collagen type I  $\alpha 1$  (*Col1a1*) and *Gata4*, a zinc finger transcription factor important for cardiac development, are often found associated with hypertrophic cardiomyopathy.<sup>37–41</sup> Although not significant ( $P = 0.092$ ), a small increase in expression of myosin heavy chain 6 (*Myh6*) in RAPA-treated mice (Fig. 5C) was also consistent with improved cardiac health, since *Myh6* has been shown to be downregulated in hypertrophic and dilated cardiomyopathy.<sup>42–44</sup> No difference in the expression of cardiac transcription factor NK2 homeobox 5 (*Nkx2-5*), was detected between groups (Fig. 5D). Cardiac type 2 deiodinase (*Dio2*) showed marginal reductions in expression in RAPA-treated mice ( $P = 0.052$ ; Fig. 5E). This result is not particularly surprising since studies have suggested that RAPA treatment of mice is able to prevent thyroid hormone induced cardiac hypertrophy.<sup>45</sup> Masson's trichrome-stained left ventricular heart sections showed significantly reduced myocardial fibrotic staining in RAPA-treated versus untreated mice (Fig. 6A and 6B) and are consistent with reduced cardiomyopathy in the RAPA-treated animals. Additionally, no significant differences in staining were observed between the RAPA-treated BKS-*Lepr<sup>db</sup>* compared with a cohort of 20-week old C57BL/6J mice (Fig. 6B) indicating effective RAPA-mediated prevention of myocardial fibrosis.

### RAPA-treatment on life span of female and male BKS-*Lepr<sup>db</sup>* mice

Recent studies by Sataranatarajan *et al.*<sup>27</sup> showed that 4-month-old female and male BKS-*Lepr<sup>db</sup>* mice fed dietary RAPA showed ~ 15.6% and ~ 13.5% reductions in median survival. Our studies using small cohorts of female and male BKS-*Lepr<sup>db</sup>* mice fed control or dietary RAPA starting at 15 weeks of age (10 mice per group) did not result in RAPA-mediated reductions in life span (Fig. 7), but rather suggested that RAPA treatment has either no effect or could marginally increase median life span in both sexes.

### Discussion

Female BKS-*Lepr<sup>db</sup>* mice fed a diet containing RAPA showed significantly reduced body weight gain compared with control-fed mice (Fig. 1A), a phenotype that was consistent with male BKS-*Lepr<sup>db</sup>* mice administered RAPA via IP injection<sup>32</sup> or dietary supplementation.<sup>28</sup>

Evaluation of body composition after the 12-week feeding study showed that approximately 23% of the weight difference between control and RAPA-treated mice was lean or fat-free mass (FFM), with the remaining component being fat mass (Fig. 1B) predominantly associated with the subcutaneous inguinal and scapular adipose tissue depots (Fig. 1C and 1D). The reduced lean mass in these mice with respect to reduced adiposity is consistent with the “quarter FFM rule” of Heymsfield *et al.*,<sup>34</sup> which is used to determine normal functional FFM loss in relation to total weight loss. Because loss of FFM in RAPA-treated mice is within expected parameters in relation to differences in body weight compared with control mice, and levels of the serum marker for muscular damage creatine kinase<sup>46</sup> were similar between treatment groups (Table 1), it is unlikely that chronic dietary RAPA treatment affects skeletal muscle mass or causes muscle damage.<sup>47</sup>

Measurements of parameters associated with glucose homeostasis showed no differences in plasma glucose or insulin or pancreatic insulin content between treatment groups (Fig. 2A, 2B and 2D). However, an ITT showed that RAPA-treated BKS-*Lepr<sup>db</sup>* mice have significantly improved insulin-mediated glucose uptake compared with untreated controls (Fig. 2C). Although chronic RAPA treatment of C57BL/6J and other strains of mice have often demonstrated exacerbated hyperglycemia,<sup>36,48,49</sup> our observations with RAPA-treated BKS-*Lepr<sup>db</sup>* female mice showed either no effect or lowering of plasma glucose with RAPA treatment and were consistent with previous studies using RAPA-treated male BKS-*Lepr<sup>db</sup>* mice.<sup>26,28,32</sup> It is likely that extensive early-onset hyperglycemia caused by inactivation of *Lepr* in these mice overwhelmingly supersedes the contribution of RAPA-mediated mechanisms that potentially contribute to elevated plasma glucose, such as delayed glucose clearance, reduced pancreatic islet mass and insulin content, and increased hepatic gluconeogenesis.<sup>8,16</sup>

Serum collected and analyzed from RAPA-treated mice at the completion of the study showed significantly reduced levels of aspartate transaminase (AST;  $P < 0.01$ ) and non-significant albeit lower levels of alanine transaminase (ALT;  $P < 0.08$ ) compared with control mice, suggesting improved hepatic function. Studies suggest that RAPA-mediated inhibition of the mTORC pathway alleviates hepatic lipid deposition and steatosis by mitigating the translation of CD36, prevention of l-tryptophan- and serotonin-mediated mTORC phosphorylation, and/or enhancing hepatic autophagy and fatty acid oxidation.<sup>11–14</sup> Analyses of urine albumin/creatinine ratios (ACR), shown to be positively associated with renal damage and diabetic nephropathy,<sup>50–52</sup> were significantly reduced by ~ 50% ( $P < 0.05$ ) in the RAPA-treated mice. It is possible that RAPA-mediated attenuation of mTORC1 activation in podocytes reduces the development of diabetic nephropathy and subsequent renal damage<sup>9,10</sup> through activation of podocyte autophagy.<sup>53–56</sup> Similar dietary RAPA-mediated reductions in ACR and improvement in kidney histology were described using NONcNZO10/LtJ (NcZ10) mice, a polygenic model of obesity and T2D.<sup>36</sup>

Rapamycin inhibition of the mTOR pathway has been shown to be protective against the development of hypertrophic and uremic cardiomyopathy,<sup>29</sup> cardiomyopathy caused by inactivation of PTEN,<sup>30</sup> and in partially nephrectomized rats treated with marinobufagenin (MGB), a profibrotic cardiotonic steroid that is elevated in patients with renal failure.<sup>31</sup> Recent studies showed that 16- to 18-week-old male BKS-*Lepr<sup>db</sup>* mice treated daily for 28

days with intraperitoneal injections of RAPA had improved cardiac function compared with control mice.<sup>32</sup> In a less invasive and longer-term treatment paradigm, 11-week-old female BKS-*Lepr<sup>db</sup>* mice fed diet supplemented with RAPA for 12 weeks showed significant reductions in left ventricular diastolic posterior wall thickness (LVPW; Fig. 3A), heart size normalized to tibia length (Fig. 3B), cardiomyocyte size (Fig. 4A and 4B), and interstitial myocardial fibrosis (Fig. 6A and 6B), suggesting reduced cardiomyopathy and improved cardiac function compared with control-fed mice. Significantly reduced expression of cardiac *Colla1* and *Gata4* (Fig. 5A and 5B) and moderately increased expression of *Myh6* (Fig. 5C), well-characterized markers for hypertrophic cardiomyopathy,<sup>37–44</sup> further support the beneficial RAPA-mediated effects in improving cardiac function. Although many studies have shown positive effects of RAPA-mediated inhibition of mTORC on cardiac health,<sup>57</sup> it has recently been suggested that dietary rapamycin can also improve age-related endothelial function and elasticity.<sup>58</sup>

In mouse models with dilated cardiomyopathy elevated cardiac type 2 deiodinase (*Dio2*)<sup>59</sup> and hyperthyroidism in syndromes such as Grave's Disease<sup>60</sup> can lead to increased hypertrophic cardiac remodeling and further worsening of cardiac function. Therefore, the borderline significant reduction of cardiac *Dio2* in mice fed dietary RAPA ( $P=0.052$ ; Fig. 5E) could be either a consequence of attenuated cardiomyopathy or caused via RAPA-mediated effects on mTORC regulation of *Dio2* and prevention of localized conversion of T4 to T3.<sup>45</sup> Further studies are needed to fully understand the complexity of mTORC signaling in mediating cardiac thyroid hormone function.

It has been widely demonstrated that mice fed diet containing low levels (14 ppm) of encapsulated RAPA have increased longevity,<sup>1,5,61</sup> and RAPA treatment can extend life span and delay tumorigenesis in genetically predisposed mouse models.<sup>62–65</sup> However, a recent study suggests that some mouse strains, such as the T2D-prone, *Lepr*-deficient BKS-*Lepr<sup>db</sup>* mice, may be at risk for increased mortality when fed dietary RAPA because of further impairment of glucose homeostasis, pancreatic islet function, and insulin secretion.<sup>27,28</sup> In a study using a smaller cohort of mice, we did not see clear evidence of increased mortality in RAPA-treated female or male mice. Although the differences in longevity between treatment groups in our studies and those of Sataranatarajan *et al.*<sup>27</sup> are not known, it is possible that differences in vivarium conditions between institutions could play a role in RAPA-mediated effects on life span.

In summary, our studies show that dietary RAPA treatment of T2D-prone female BKS-*Lepr<sup>db</sup>* mice leads to reduced adiposity, improved insulin sensitivity, and improved cardiac health and function compared with mice fed a control diet. Knowledge gained from these studies and those of others can be applied to polygenic animal models susceptible to the development of obesity, T2D, and cardiomyopathy to further profile the impact and mechanistic aspects of RAPA-mediated mTORC inhibition on the progression of metabolic disease and overall effects on health span.

## Acknowledgments

Support was provided by the Molecular Phenotyping (supported by P30GM106391 and U54GM115516) and Histopathology and Histomorphometry (supported by P30GM106391, P30GM103392, P20GM121301, and



U54GM115516) cores at the Maine Medical Center Research Institute and NIH Grant AG022308 at the Jackson Laboratory. The authors wish to thank Clinton M. Astle for help procuring the diets and Vicki Ingalls, Nelson Durgin, and Leonor Robidoux for excellent care and maintenance of the mice.

## References

1. Harrison DE, Strong R, Sharp ZD, et al. Rapamycin fed late in life extends lifespan in genetically heterogeneous mice. *Nature*. 2009; 460:392–395. [PubMed: 19587680]
2. Jia K, Chen D, Riddle DL. The TOR pathway interacts with the insulin signaling pathway to regulate *C. elegans* larval development, metabolism and life span. *Development*. 2004; 131:3897–3906. [PubMed: 15253933]
3. Powers RW 3rd, Kaerberlein M, Caldwell SD, et al. Extension of chronological life span in yeast by decreased TOR pathway signaling. *Genes & development*. 2006; 20:174–184. [PubMed: 16418483]
4. Vellai T, Takacs-Vellai K, Zhang Y, et al. Genetics: influence of TOR kinase on lifespan in *C. elegans*. *Nature*. 2003; 426:620.
5. Wilkinson JE, Burmeister L, Brooks SV, et al. Rapamycin slows aging in mice. *Aging cell*. 2012; 11:675–682. [PubMed: 22587563]
6. Chang GR, Chiu YS, Wu YY, et al. Rapamycin protects against high fat diet-induced obesity in C57BL/6J mice. *Journal of pharmacological sciences*. 2009; 109:496–503. [PubMed: 19372632]
7. Chang GR, Wu YY, Chiu YS, et al. Long-term administration of rapamycin reduces adiposity, but impairs glucose tolerance in high-fat diet-fed KK/HIJ mice. *Basic & clinical pharmacology & toxicology*. 2009; 105:188–198. [PubMed: 19496779]
8. Houde VP, Brule S, Festuccia WT, et al. Chronic rapamycin treatment causes glucose intolerance and hyperlipidemia by upregulating hepatic gluconeogenesis and impairing lipid deposition in adipose tissue. *Diabetes*. 2010; 59:1338–1348. [PubMed: 20299475]
9. Inoki K, Mori H, Wang J, et al. mTORC1 activation in podocytes is a critical step in the development of diabetic nephropathy in mice. *The Journal of clinical investigation*. 2011; 121:2181–2196. [PubMed: 21606597]
10. Zschiedrich S, Bork T, Liang W, et al. Targeting mTOR Signaling Can Prevent the Progression of FSGS. *Journal of the American Society of Nephrology : JASN*. 2017; 28:2144–2157. [PubMed: 28270414]
11. Liu TY, Xiong XQ, Ren XS, et al. FNDC5 Alleviates Hepatosteatosis by Restoring AMPK/mTOR-Mediated Autophagy, Fatty Acid Oxidation, and Lipogenesis in Mice. *Diabetes*. 2016; 65:3262–3275. [PubMed: 27504012]
12. Nakadera E, Yamashina S, Izumi K, et al. Inhibition of mTOR improves the impairment of acidification in autophagic vesicles caused by hepatic steatosis. *Biochemical and biophysical research communications*. 2016; 469:1104–1110. [PubMed: 26687947]
13. Osawa Y, Kanamori H, Seki E, et al. L-tryptophan-mediated enhancement of susceptibility to nonalcoholic fatty liver disease is dependent on the mammalian target of rapamycin. *J Biol Chem*. 2011; 286:34800–34808. [PubMed: 21841000]
14. Wang C, Yan Y, Hu L, et al. Rapamycin-mediated CD36 translational suppression contributes to alleviation of hepatic steatosis. *Biochemical and biophysical research communications*. 2014; 447:57–63. [PubMed: 24685479]
15. Lamming DW, Ye L, Astle CM, et al. Young and old genetically heterogeneous HET3 mice on a rapamycin diet are glucose intolerant but insulin sensitive. *Aging cell*. 2013; 12:712–718. [PubMed: 23648089]
16. Yang SB, Lee HY, Young DM, et al. Rapamycin induces glucose intolerance in mice by reducing islet mass, insulin content, and insulin sensitivity. *Journal of molecular medicine*. 2012; 90:575–585. [PubMed: 22105852]
17. Lew S, Chamberlain RS. Risk of Metabolic Complications in Patients with Solid Tumors Treated with mTOR inhibitors: Meta-analysis. *Anticancer research*. 2016; 36:1711–1718. [PubMed: 27069150]

18. Morrisett JD, Abdel-Fattah G, Hoogeveen R, et al. Effects of sirolimus on plasma lipids, lipoprotein levels, and fatty acid metabolism in renal transplant patients. *J Lipid Res.* 2002; 43:1170–1180. [PubMed: 12177161]
19. Barlow AD, Xie J, Moore CE, et al. Rapamycin toxicity in MIN6 cells and rat and human islets is mediated by the inhibition of mTOR complex 2 (mTORC2). *Diabetologia.* 2012; 55:1355–1365. [PubMed: 22314813]
20. Lamming DW, Ye L, Katajisto P, et al. Rapamycin-induced insulin resistance is mediated by mTORC2 loss and uncoupled from longevity. *Science.* 2012; 335:1638–1643. [PubMed: 22461615]
21. Volkers M, Konstandin MH, Doroudgar S, et al. Mechanistic target of rapamycin complex 2 protects the heart from ischemic damage. *Circulation.* 2013; 128:2132–2144. [PubMed: 24008870]
22. Volkers M, Doroudgar S, Nguyen N, et al. PRAS40 prevents development of diabetic cardiomyopathy and improves hepatic insulin sensitivity in obesity. *EMBO molecular medicine.* 2014; 6:57–65. [PubMed: 24408966]
23. Das A, Salloum FN, Filippone SM, et al. Inhibition of mammalian target of rapamycin protects against reperfusion injury in diabetic heart through STAT3 signaling. *Basic research in cardiology.* 2015; 110:31. [PubMed: 25911189]
24. Filippone SM, Samidurai A, Roh SK, et al. Reperfusion Therapy with Rapamycin Attenuates Myocardial Infarction through Activation of AKT and ERK. *Oxidative medicine and cellular longevity.* 2017; 2017:4619720. [PubMed: 28373901]
25. Barlow AD, Nicholson ML, Herbert TP. Evidence for rapamycin toxicity in pancreatic beta-cells and a review of the underlying molecular mechanisms. *Diabetes.* 2013; 62:2674–2682. [PubMed: 23881200]
26. Deepa SS, Walsh ME, Hamilton RT, et al. Rapamycin Modulates Markers of Mitochondrial Biogenesis and Fatty Acid Oxidation in the Adipose Tissue of db/db Mice. *Journal of biochemical and pharmacological research.* 2013; 1:114–123. [PubMed: 24010023]
27. Sataranatarajan K, Ikeno Y, Bokov A, et al. Rapamycin Increases Mortality in db/db Mice, a Mouse Model of Type 2 Diabetes. *The journals of gerontology. Series A, Biological sciences and medical sciences.* 2016; 71:850–857.
28. Reifsnnyder PC, Flurkey K, Te A, et al. Rapamycin treatment benefits glucose metabolism in mouse models of type 2 diabetes. *Aging.* 2016; 8:3120–3130. [PubMed: 27922820]
29. Marin TM, Keith K, Davies B, et al. Rapamycin reverses hypertrophic cardiomyopathy in a mouse model of LEOPARD syndrome-associated PTPN11 mutation. *The Journal of clinical investigation.* 2011; 121:1026–1043. [PubMed: 21339643]
30. Xu X, Roe ND, Weiser-Evans MC, et al. Inhibition of mammalian target of rapamycin with rapamycin reverses hypertrophic cardiomyopathy in mice with cardiomyocyte-specific knockout of PTEN. *Hypertension.* 2014; 63:729–739. [PubMed: 24446058]
31. Haller ST, Yan Y, Drummond CA, et al. Rapamycin Attenuates Cardiac Fibrosis in Experimental Uremic Cardiomyopathy by Reducing Marinobufagenin Levels and Inhibiting Downstream Pro-Fibrotic Signaling. *Journal of the American Heart Association.* 2016; 5
32. Das A, Durrant D, Koka S, et al. Mammalian target of rapamycin (mTOR) inhibition with rapamycin improves cardiac function in type 2 diabetic mice: potential role of attenuated oxidative stress and altered contractile protein expression. *J Biol Chem.* 2014; 289:4145–4160. [PubMed: 24371138]
33. Nikonova L, Koza RA, Mendoza T, et al. Mesoderm-specific transcript is associated with fat mass expansion in response to a positive energy balance. *FASEB journal : official publication of the Federation of American Societies for Experimental Biology.* 2008; 22:3925–3937. [PubMed: 18644838]
34. Heymsfield SB, Gonzalez MC, Shen W, et al. Weight loss composition is one-fourth fat-free mass: a critical review and critique of this widely cited rule. *Obesity reviews : an official journal of the International Association for the Study of Obesity.* 2014; 15:310–321. [PubMed: 24447775]
35. Hummel KP, Dickie MM, Coleman DL. Diabetes, a new mutation in the mouse. *Science.* 1966; 153:1127–1128. [PubMed: 5918576]

36. Reifsnyder PC, Doty R, Harrison DE. Rapamycin ameliorates nephropathy despite elevating hyperglycemia in a polygenic mouse model of type 2 diabetes, NONcNZO10/LtJ. *PLoS One*. 2014; 9:e114324. [PubMed: 25473963]
37. Diao X, Shen E, Wang X, et al. Differentially expressed microRNAs and their target genes in the hearts of streptozotocin-induced diabetic mice. *Mol Med Rep*. 2011; 4:633–640. [PubMed: 21584493]
38. Fang CX, Dong F, Thomas DP, et al. Hypertrophic cardiomyopathy in high-fat diet-induced obesity: role of suppression of forkhead transcription factor and atrophy gene transcription. *Am J Physiol Heart Circ Physiol*. 2008; 295:H1206–H1215. [PubMed: 18641278]
39. Kwon DH, Eom GH, Kee HJ, et al. Estrogen-related receptor gamma induces cardiac hypertrophy by activating GATA4. *Journal of molecular and cellular cardiology*. 2013; 65:88–97. [PubMed: 24083978]
40. Liang Q, De Windt LJ, Witt SA, et al. The transcription factors GATA4 and GATA6 regulate cardiomyocyte hypertrophy in vitro and in vivo. *J Biol Chem*. 2001; 276:30245–30253. [PubMed: 11356841]
41. Tsybouleva N, Zhang L, Chen S, et al. Aldosterone, through novel signaling proteins, is a fundamental molecular bridge between the genetic defect and the cardiac phenotype of hypertrophic cardiomyopathy. *Circulation*. 2004; 109:1284–1291. [PubMed: 14993121]
42. Barth AS, Kuner R, Bunes A, et al. Identification of a common gene expression signature in dilated cardiomyopathy across independent microarray studies. *Journal of the American College of Cardiology*. 2006; 48:1610–1617. [PubMed: 17045896]
43. Carniel E, Taylor MR, Sinagra G, et al. Alpha-myosin heavy chain: a sarcomeric gene associated with dilated and hypertrophic phenotypes of cardiomyopathy. *Circulation*. 2005; 112:54–59. [PubMed: 15998695]
44. England J, Loughna S. Heavy and light roles: myosin in the morphogenesis of the heart. *Cellular and molecular life sciences : CMLS*. 2013; 70:1221–1239. [PubMed: 22955375]
45. Kuzman JA, O'Connell TD, Gerdes AM. Rapamycin prevents thyroid hormone-induced cardiac hypertrophy. *Endocrinology*. 2007; 148:3477–3484. [PubMed: 17395699]
46. Brancaccio P, Lippi G, Maffulli N. Biochemical markers of muscular damage. *Clinical chemistry and laboratory medicine*. 2010; 48:757–767. [PubMed: 20518645]
47. Ye L, Widlund AL, Sims CA, et al. Rapamycin doses sufficient to extend lifespan do not compromise muscle mitochondrial content or endurance. *Aging*. 2013; 5:539–550. [PubMed: 23929887]
48. Arriola Apelo SI, Neuman JC, Baar EL, et al. Alternative rapamycin treatment regimens mitigate the impact of rapamycin on glucose homeostasis and the immune system. *Aging cell*. 2016; 15:28–38. [PubMed: 26463117]
49. Liu Y, Diaz V, Fernandez E, et al. Rapamycin-induced metabolic defects are reversible in both lean and obese mice. *Aging*. 2014; 6:742–754. [PubMed: 25324470]
50. Aoki T, Kaneko S, Tanimoto M, et al. Identification of quantitative trait loci for diabetic nephropathy in KK-Ay/Ta mice. *Journal of nephrology*. 2012; 25:127–136. [PubMed: 21725918]
51. Brosius FC 3rd, Alpers CE, Bottinger EP, et al. Mouse models of diabetic nephropathy. *Journal of the American Society of Nephrology : JASN*. 2009; 20:2503–2512. [PubMed: 19729434]
52. Glastras SJ, Chen H, Teh R, et al. Mouse Models of Diabetes, Obesity and Related Kidney Disease. *PLoS One*. 2016; 11:e0162131. [PubMed: 27579698]
53. Kitada M, Ogura Y, Monno I, et al. Regulating Autophagy as a Therapeutic Target for Diabetic Nephropathy. *Current diabetes reports*. 2017; 17:53. [PubMed: 28593583]
54. Kume S, Koya D. Autophagy: A Novel Therapeutic Target for Diabetic Nephropathy. *Diabetes & metabolism journal*. 2015; 39:451–460. [PubMed: 26706914]
55. Xiao T, Guan X, Nie L, et al. Rapamycin promotes podocyte autophagy and ameliorates renal injury in diabetic mice. *Molecular and cellular biochemistry*. 2014; 394:145–154. [PubMed: 24850187]
56. Xin W, Li Z, Xu Y, et al. Autophagy protects human podocytes from high glucose-induced injury by preventing insulin resistance. *Metabolism: clinical and experimental*. 2016; 65:1307–1315. [PubMed: 27506738]

57. Xu L, Brink M. mTOR, cardiomyocytes and inflammation in cardiac hypertrophy. *Biochimica et biophysica acta*. 2016; 1863:1894–1903. [PubMed: 26775585]
58. Lesniewski LA, Seals DR, Walker AE, et al. Dietary rapamycin supplementation reverses age-related vascular dysfunction and oxidative stress, while modulating nutrient-sensing, cell cycle, and senescence pathways. *Aging cell*. 2017; 16:17–26. [PubMed: 27660040]
59. Wang YY, Morimoto S, Du CK, et al. Up-regulation of type 2 iodothyronine deiodinase in dilated cardiomyopathy. *Cardiovascular research*. 2010; 87:636–646. [PubMed: 20453157]
60. Ertek S, Cicero AF. Hyperthyroidism and cardiovascular complications: a narrative review on the basis of pathophysiology. *Archives of medical science : AMS*. 2013; 9:944–952. [PubMed: 24273583]
61. Miller RA, Harrison DE, Astle CM, et al. Rapamycin, but not resveratrol or simvastatin, extends life span of genetically heterogeneous mice. *The journals of gerontology. Series A, Biological sciences and medical sciences*. 2011; 66:191–201.
62. Anisimov VN, Zabezhinski MA, Popovich IG, et al. Rapamycin extends maximal life span in cancer-prone mice. *The American journal of pathology*. 2010; 176:2092–2097. [PubMed: 20363920]
63. Anisimov VN, Zabezhinski MA, Popovich IG, et al. Rapamycin increases lifespan and inhibits spontaneous tumorigenesis in inbred female mice. *Cell cycle*. 2011; 10:4230–4236. [PubMed: 22107964]
64. Komarova EA, Antoch MP, Novototskaya LR, et al. Rapamycin extends lifespan and delays tumorigenesis in heterozygous p53+/- mice. *Aging*. 2012; 4:709–714. [PubMed: 23123616]
65. Livi CB, Hardman RL, Christy BA, et al. Rapamycin extends life span of Rb1+/- mice by inhibiting neuroendocrine tumors. *Aging*. 2013; 5:100–110. [PubMed: 23454836]

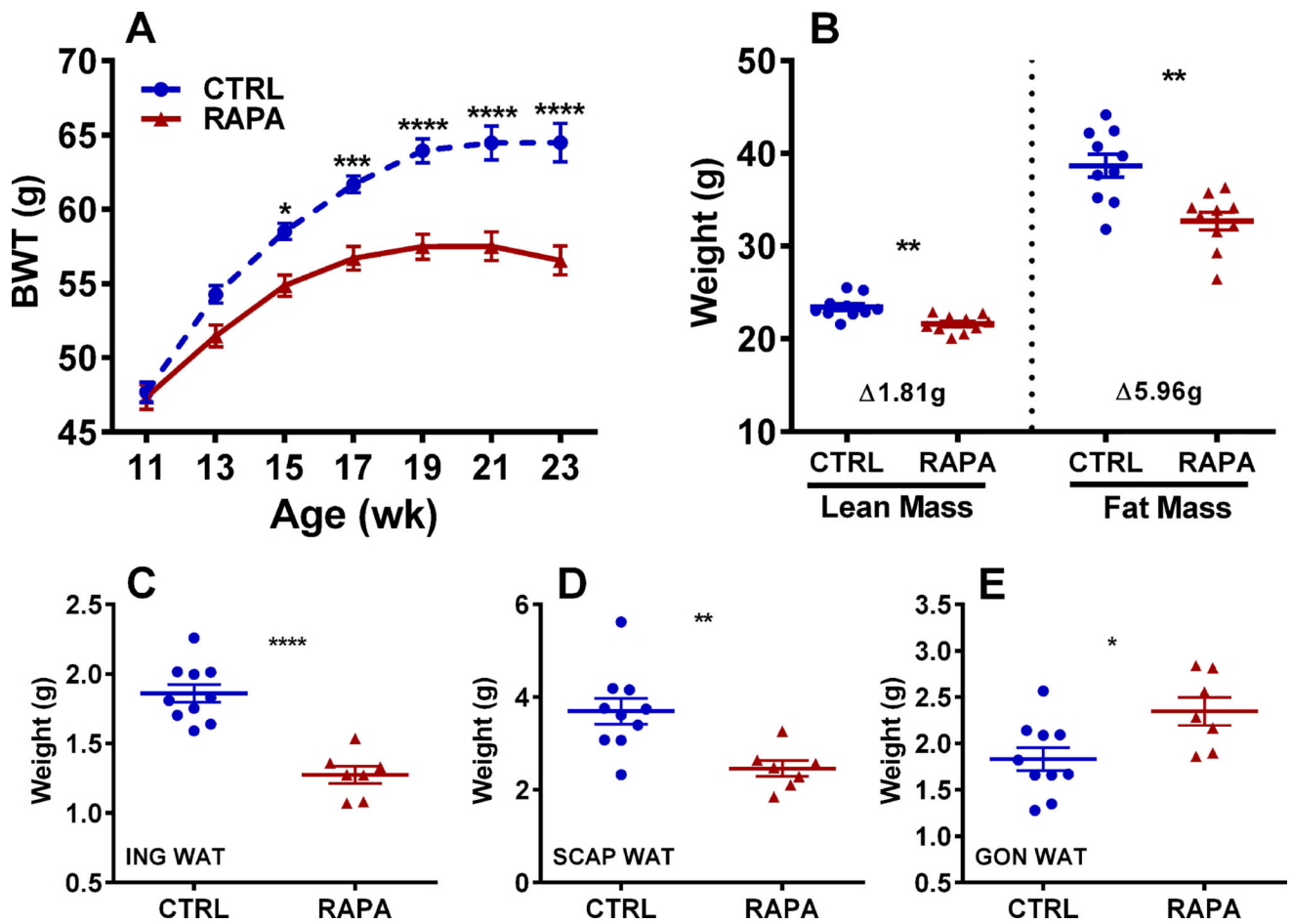


**Figure 1.**

Data represents longitudinal measurements of bodyweight at the age indicated (BWT; A) and body composition measured at 24 weeks of age (B) for 10 control (CTRL) and 10 rapamycin-treated (RAPA) female BKS-*Lepr<sup>db</sup>* mice. Weights of inguinal (ING; C), scapular (SCAP; D) and gonadal (GON; E) white adipose tissue (WAT) were measured at 27 weeks of age in 10 CTRL and 7 RAPA mice. Significance between groups in A was measured using 2-way ANOVA with Sidak's multiple comparisons test and in B-E using two-tailed unpaired parametric *t*-tests. Data sets annotated with 1, 2, 3 or 4 asterisks indicate significant *P* values of < 0.05, < 0.01, < 0.001, and < 0.0001.

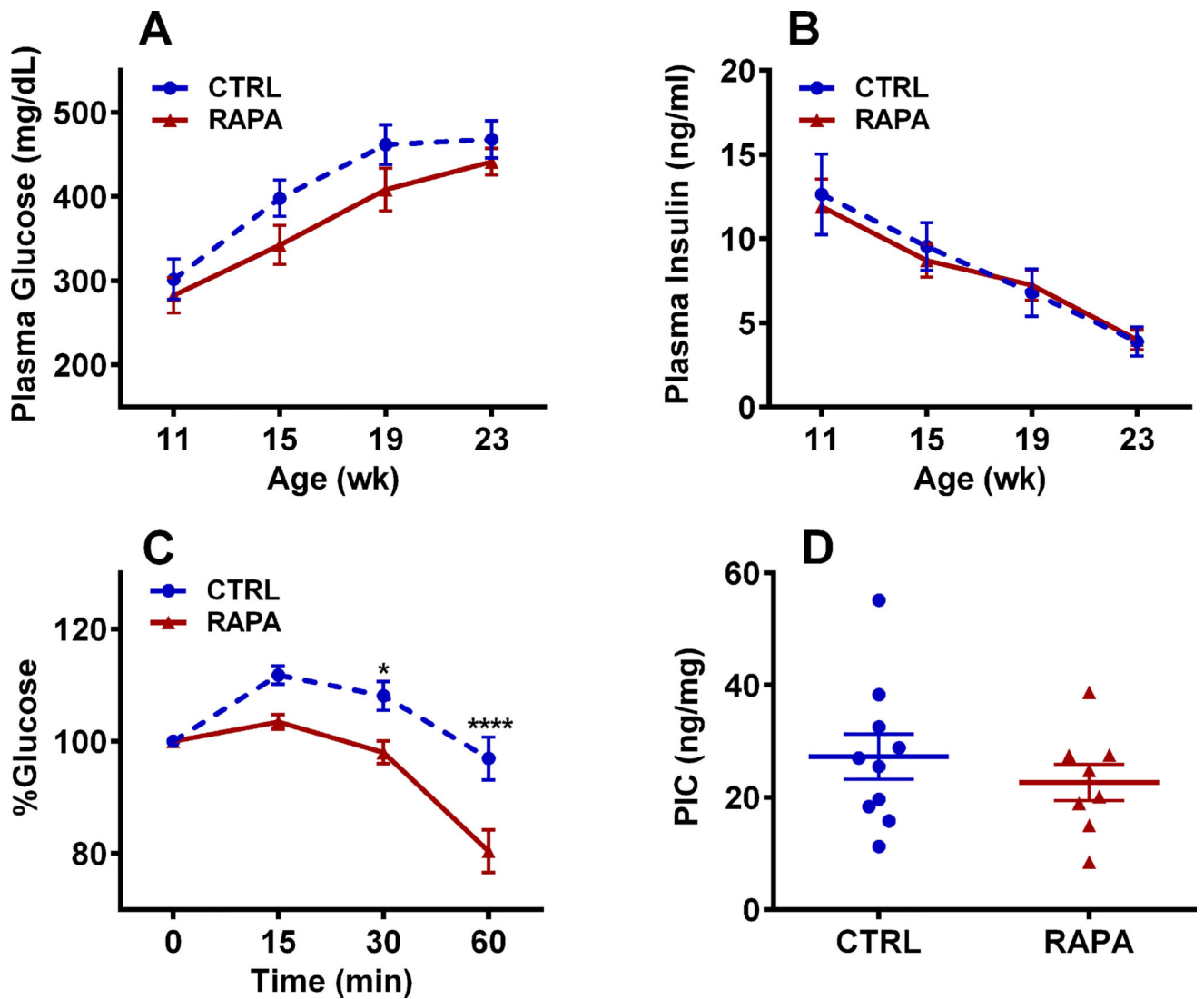


**Figure 2.**

Data represents longitudinal measurements of (A) plasma glucose and (B) insulin at the ages indicated for 10 control (CTRL) and 10 rapamycin-treated (RAPA) female BKS-*Lepr<sup>db</sup>* mice. (C) Insulin tolerance test of 10 CTRL and 10 RAPA mice at 24 weeks of age. (D) Measurements of pancreatic insulin content (PIC) of 10 CTRL and 7 RAPA mice at 27 weeks of age. Significance between groups in A–C was measured using 2-way ANOVA with Sidak's multiple comparisons test and in D using two-tailed unpaired parametric t-tests. Data sets annotated with 1 or 4 asterisks indicate significant *P* values of < 0.05 and < 0.0001.

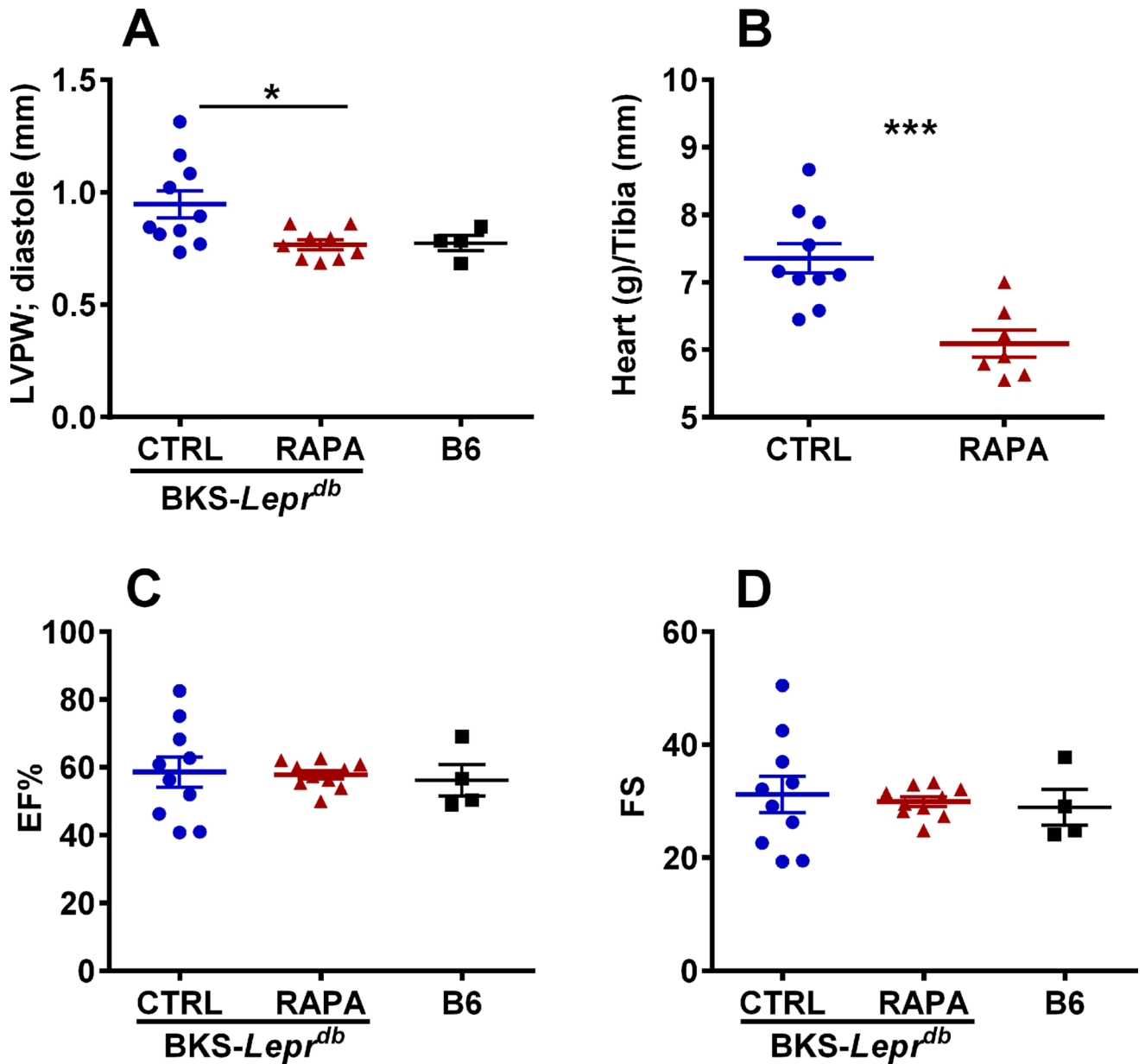


**Figure 3.**

(A) Data represents echocardiography measurements of left ventricular posterior wall (LVPW) thickness measured at 25 weeks of age for 10 control (CTRL) and 10 rapamycin-treated (RAPA) female BKS-*Lepr*<sup>db</sup> mice and four 8-week old female C57BL/6J mice. (B) Heart weight normalized to tibia length in 10 CTRL and 7 RAPA mice at 27 weeks of age. (C and D) Echocardiography measurements of ejection fraction (EF%) and fractional shortening (FS). Significance between groups was analyzed using two-tailed unpaired parametric t-tests. Data sets annotated with 1 or 3 asterisks indicate significant *P* values of < 0.05 and < 0.001.

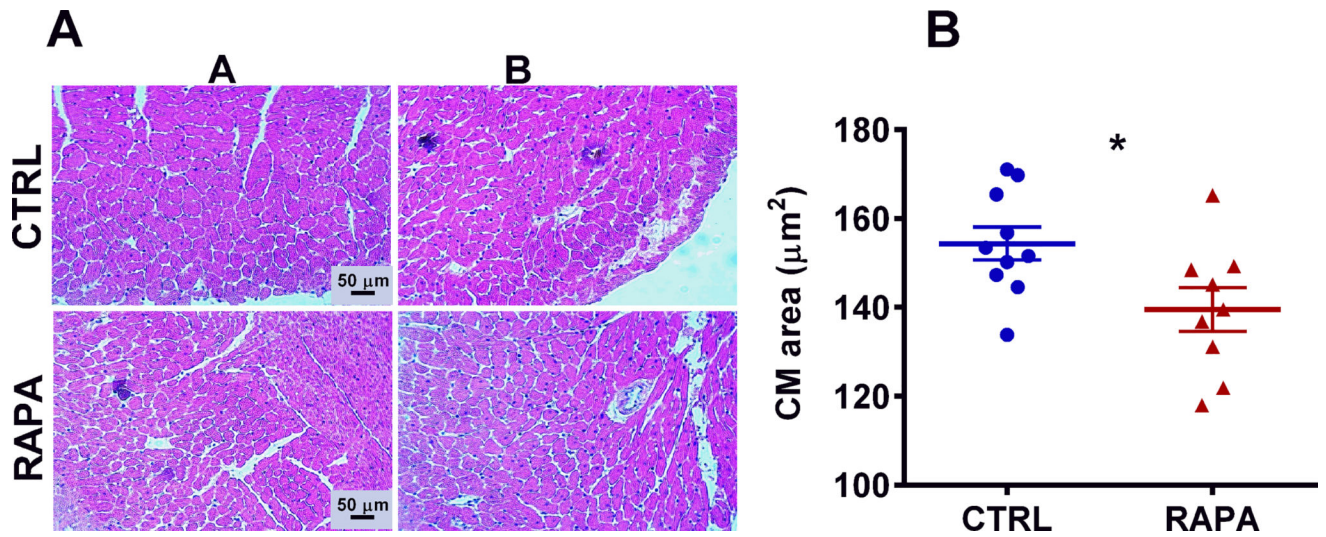


**Figure 4.** Data represents histomorphometric analyses of cardiomyocyte (CM) size in mice at 27 weeks of age. (A) Representative H&E-stained images of control untreated (CTRL) and RAPA-treated BKS-*Lepr<sup>db</sup>* mice. (B) Quantitative results for cardiomyocyte size in 10 CTRL and 9 RAPA-treated mice. Significance between groups was analyzed using two-tailed unpaired parametric *t*-tests. Data annotated with an asterisk indicates a *P* value of < 0.05.



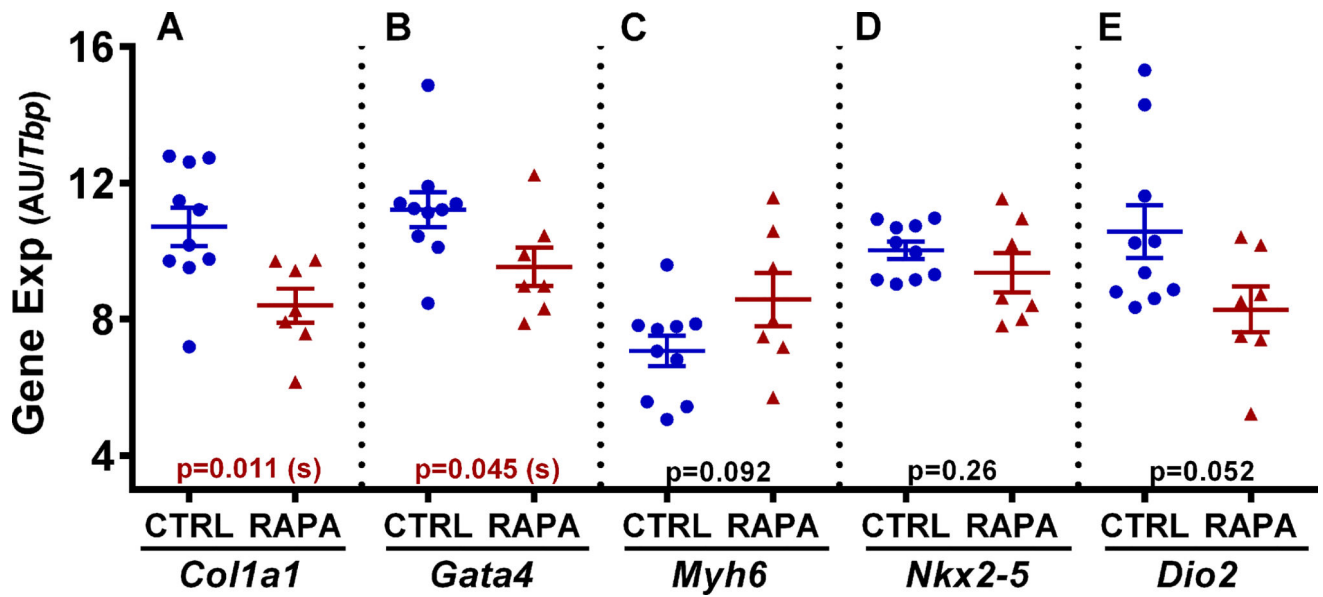


**Figure 5.**

Data in A–E show the analyses of heart-derived RNA from 10 control (CTRL) and 7 rapamycin-treated (RAPA) female BKS-*Lepr<sup>db</sup>* mice for each of the genes indicated below each panel. Gene expression was measured by TaqMan QRT-PCR and is represented as arbitrary units (AU) normalized to TATA-box binding protein (*Tbp*). Significance between groups was analyzed using two-tailed unpaired parametric *t*-tests and *P* values are indicated within each panel.

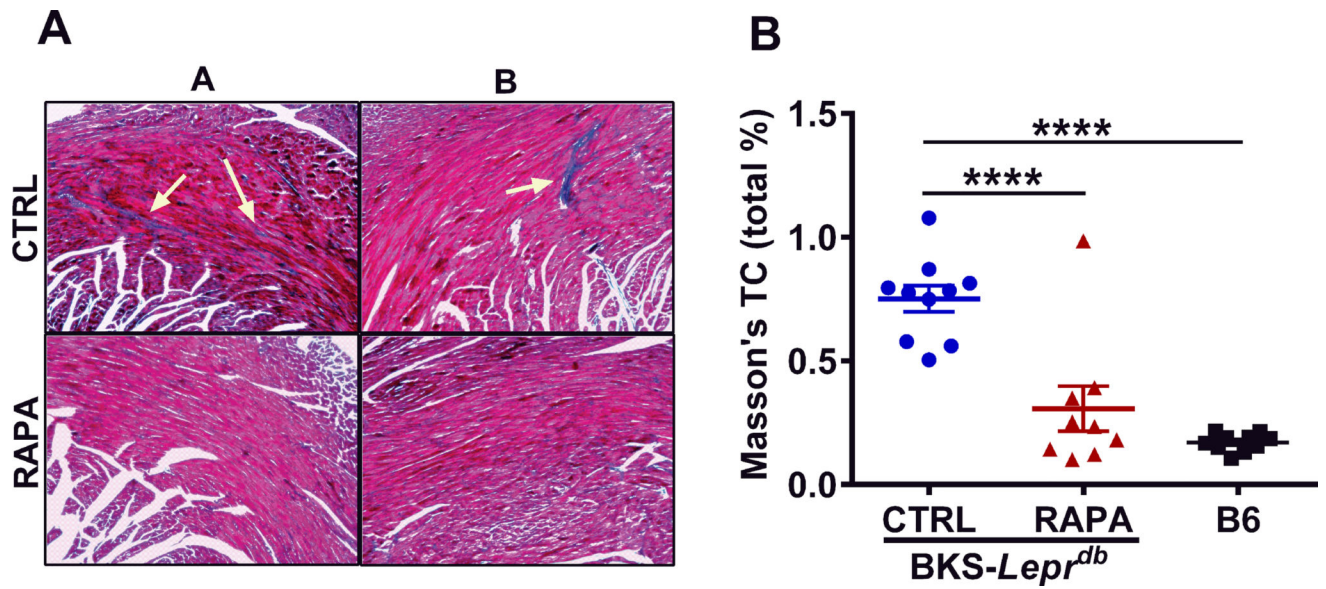


**Figure 6.**

Data represents histomorphometric analyses of interstitial myocardial fibrosis via Masson's trichrome staining of left ventricular heart sections from mice at 27 weeks of age. (A) Representative Masson's trichrome-stained images of control untreated (CTRL) and RAPA-treated BKS-*Lepr<sup>db</sup>* mice. Arrows indicate fibrotic regions that are stained blue. (B) Quantitative analyses of Masson's trichrome staining of fibrosis in CTRL ( $n = 10$ ) and RAPA-treated ( $n = 9$ ) BKS-*Lepr<sup>db</sup>* mice as well as 20-week-old C57BL/6J (B6) mice ( $n = 10$ ) from an independent cohort. Significance among multiple groups was calculated with ordinary one-way ANOVA followed by Tukey's multiple comparisons test with an  $\alpha$  of 0.5. Data annotated with four asterisks indicates a  $P$  value of  $< 0.0001$ .

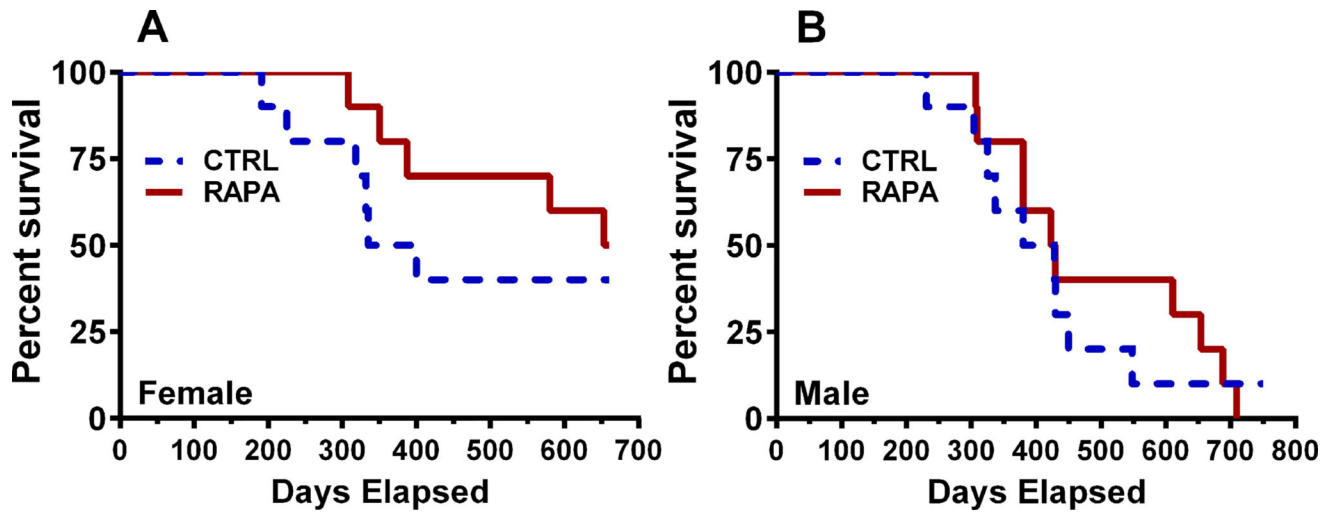


**Figure 7.**

Data represents survival curves for (A) 10 control (CTRL) and 10 rapamycin-treated (RAPA) female BKS-*LepI<sup>db</sup>* mice and (B) 10 CTRL and 10-RAPA male BKS-*LepI<sup>db</sup>* mice. Mice were placed on non-supplemented and encapsulated RAPA (14 ppm)-supplemented dietary treatment at 15 weeks of age.

**Table 1**

Serum parameters of control and rapamycin treated female *Lep<sup>r<sup>db</sup></sup>* mice.

Serum parameter	CTRL ( <i>n</i> = 10)	RAPA ( <i>n</i> = 7)	<i>P</i> value
GLU (mg/dL)	633 ± 28.4	497 ± 26.2	<b>0.0042</b>
TRIG (mg/dL)	242 ± 18.3	208 ± 20.9	0.24
BUN (mg/dL)	20.0 ± 0.73	18.9 ± 0.91	0.34
ALT (IU/L)	98.4 ± 12.8	62.6 ± 13.3	0.078
AST (IU/L)	137 ± 14.0	80.3 ± 10.3	<b>0.0091</b>
T4 (ug/dL)	4.29 ± 0.10	4.80 ± 0.19	<b>0.019</b>
TUP (%)	34.9 ± 4.16	37.0 ± 5.82	0.76
CK (IU/L)	169 ± 64.2	172 ± 47.1	0.97

NOTE: Significance between groups was analyzed using two-tailed unpaired parametric *t*-tests and significant *P* values are indicated in bold. GLU, glucose; TRIG, triglyceride; BUN, blood urea nitrogen; ALT, alanine transaminase; AST, aspartate transaminase; T4, thyroxine; TUP (%), thyroxine uptake; CK, creatine kinase.

Author Manuscript

Author Manuscript

Author Manuscript

Author Manuscript